

# The fundamental difference between shear alpha-viscosity and turbulent magnetorotational stresses

Martin E. Pessah<sup>1,3,4\*</sup>, Chi-kwan Chan<sup>2,4</sup>, and Dimitrios Psaltis<sup>3,4</sup>

<sup>1</sup>*Institute for Advanced Study, School of Natural Sciences, Einstein Drive, Princeton, NJ, 08540, USA*

<sup>2</sup>*Institute for Theory and Computation, Harvard-Smithsonian Center for Astrophysics, 60 Garden Street, Cambridge, MA 02138, USA*

<sup>3</sup>*Astronomy Department, 933 N. Cherry Ave., Tucson, AZ, 85721, USA*

<sup>4</sup>*Physics Department, 1118 E. 4<sup>th</sup> St., Tucson, AZ, 85721, USA*

Accepted — . Received — ; in original form —

## ABSTRACT

Numerical simulations of turbulent, magnetized, differentially rotating flows driven by the magnetorotational instability are often used to calculate the effective values of alpha viscosity that is invoked in analytical models of accretion discs. In this paper we use various dynamical models of turbulent magnetohydrodynamic stresses, as well as numerical simulations of shearing boxes, to show that angular momentum transport in MRI-driven accretion discs cannot be described by the standard model for shear viscosity. In particular, we demonstrate that turbulent magnetorotational stresses are not linearly proportional to the local shear and vanish identically for angular velocity profiles that increase outwards.

**Key words:** black hole physics – accretion, accretion discs – MHD – instability – turbulence.

## 1 INTRODUCTION

It has long been recognized that molecular viscosity cannot be solely responsible for angular momentum transport in accretion discs. Shakura & Sunyaev (1973) offered an appealing solution to this problem by postulating a source of enhanced disc viscosity due to turbulence and magnetic fields. The standard accretion disc model rests on the idea that the stresses between adjacent disc annuli are proportional to the local shear, as in a Newtonian laminar shear flow, but that it is the interaction of large turbulent eddies that results in efficient transport. The idea that turbulent angular momentum transfer in accretion discs can be described in terms of an enhanced version of the molecular transport operating in (laminar) differentially rotating media has been at the core of the majority of studies in accretion disc theory and phenomenology ever since (see, e.g., Frank, King, & Raine 2002).

The origin of the turbulence that leads to enhanced angular momentum transport in accretion discs has been a matter of debate since the work of Shakura & Sunyaev (1973). The issue of whether hydrodynamic turbulence can be generated and sustained in astrophysical discs, due to the large Reynolds numbers involved, is currently a matter of renewed interest (Afshordi, Mukhopadhyay, & Narayan 2005; Mukhopadhyay, Afshordi, & Narayan 2005). However, this idea has long been challenged by analytical (Ryu & Goodman 1992; Balbus & Hawley 2006), numerical (Stone & Balbus 1996; Balbus, Hawley, & Stone 1996; Balbus & Hawley 1997;

Hawley, Balbus, & Winters 1999), and, more recently, experimental work (Ji, Burin, Schartman, & Goodman 2006).

During the last decade, it has become evident that the interplay between turbulence and magnetic fields is at a more fundamental level than originally conceived. There is now strong theoretical and numerical evidence suggesting that the process driving the turbulence in accretion discs is related to a magnetic instability that operates in the presence of a radially decreasing angular velocity profile. Since the appreciation of the relevance of this magnetorotational instability (MRI) to accretion physics (Balbus & Hawley 1991; see also Balbus & Hawley 1998 and Balbus 2003 for a more recent review), a variety of local (Hawley, Gammie, & Balbus 1995, 1996; Stone, Hawley, Gammie, & Balbus 1996; Brandenburg, Nordlund, Stein, & Torkelsson 1995; Brandenburg 2001; Sano, Inutsuka, Turner, & Stone 2004) and global (Armitage 1998; Hawley 2000, 2001; Hawley & Krolik 2001; Stone & Pringle 2001) numerical simulations have revealed that its long-term evolution gives rise to a turbulent state and provides a natural avenue for vigorous angular momentum transport.

The fact that the overall energetic properties of turbulent magnetohydrodynamic (MHD) accretion discs are similar to those of viscous accretion discs (Balbus & Papaloizou 1999) has led to the notion that angular momentum transport due to MRI-driven turbulence in rotating shearing flows can be described in terms of the alpha model proposed by Shakura & Sunyaev (1973). This, in turn, has motivated many efforts aimed to computing effective alpha values from numerical simulations (see, e.g., Gammie 1998; Brandenburg 1998, and references therein) in order to use them in large scale analytical models of accretion discs.

In this paper, we address in detail how the transport of angular

\* E-mail: mpessah@ias.edu (MEP)

momentum mediated by MHD turbulence depends on the magnitude of the local disc shear and contrast this result to the standard model for shear viscosity. We find that one of the fundamental assumptions in which the standard viscous disc model is based, i.e., that angular momentum transport is linearly proportional to the local shear, is not appropriate for describing turbulent MRI-driven accretion discs.

## 2 ALPHA VISCOSITY VS. TURBULENT MHD STRESSES

The equation describing the dynamical evolution of the mean angular momentum density of a fluid element,  $\bar{l}$ , in an axisymmetric, turbulent MHD accretion disc with tangled magnetic fields is

$$\frac{\partial \bar{l}}{\partial t} + \frac{1}{r} \frac{\partial}{\partial r} (r \bar{l} \bar{v}_r) = -\frac{1}{r} \frac{\partial}{\partial r} (r^2 \bar{T}_{r\phi}). \quad (1)$$

Here, the over-bars denote properly averaged values (see, e.g., Balbus & Hawley 1998; Balbus & Papaloizou 1999),  $\bar{v}_r$  is the radial mean flow velocity, and the quantity  $\bar{T}_{r\phi}$  represents the total stress

$$\bar{T}_{r\phi} \equiv \bar{R}_{r\phi} - \bar{M}_{r\phi} \quad (2)$$

acting on a fluid element as a result of the correlated fluctuations in the velocity and magnetic fields in the turbulent flow, i.e.,

$$\bar{R}_{r\phi} \equiv \langle \rho \delta v_r \delta v_\phi \rangle, \quad (3)$$

$$\bar{M}_{r\phi} \equiv \frac{\langle \delta B_r \delta B_\phi \rangle}{4\pi}, \quad (4)$$

where  $\bar{R}_{r\phi}$  and  $\bar{M}_{r\phi}$  stand for the  $r\phi$ -components of the Reynolds and Maxwell stress tensors, respectively.

Equation (1) highlights the all-important role played by correlated velocity and magnetic-field fluctuations in turbulent accretion discs; if they vanish, the mean angular momentum density of a fluid element is conserved. In order for matter in the bulk of the disc to accrete, i.e., to lose angular momentum, the sign of the mean total stress must be positive. Note that the potential for correlated kinetic fluctuations to transport angular momentum in unmagnetized discs is still present in the hydrodynamic version of equation (1). However, the dynamical role played by the correlated velocity fluctuations in hydrodynamic flows is radically different from the corresponding role played by correlated velocity and magnetic field fluctuations in MHD flows, even when the magnetic fields involved are weak (Balbus & Hawley 1997, 1998).

In order to calculate the structure of an accretion disc for which angular momentum flows according to equation (1), it is necessary to obtain a closed system of equations for the second-order correlations defining the total stress  $\bar{T}_{r\phi}$ . In this context, the original proposal by Shakura and Sunyaev (see also, Lynden-Bell & Pringle 1974) can be seen as a simple closure scheme for the correlations defining the total turbulent stress in terms of mean flow variables (e.g., the pressure).

The model for angular momentum transport on which the standard accretion disc is based rests on two distinct assumptions. First, it is postulated that the vertically averaged stress exerted on any given disc annulus can be modeled as a shear viscous stress (Lynden-Bell & Pringle 1974), i.e., in cylindrical coordinates,

$$\bar{T}_{r\phi}^v \equiv -r \Sigma \nu_{\text{turb}} \frac{d\Omega}{dr}, \quad (5)$$

where  $\Sigma$  and  $\Omega$  stand for the vertically integrated disc density and the angular velocity at the radius  $r$ , respectively. This is a modifica-

tion of the Newtonian model for the viscous stress between adjacent layers in a differentially rotating laminar flow (Landau & Lifshitz 1959); in this case, the coefficient  $\nu_{\text{turb}}$  parametrizes the turbulent kinematic viscosity. In this model, the direction of angular momentum transport is always opposite to the angular velocity gradient. This is the essence of a shear-driven viscous disc.

Second, on dimensional grounds, it is assumed that the viscosity coefficient can be parametrized as  $\nu_{\text{turb}} \equiv \alpha c_s H$ . This is because the physical mechanism that allows for angular momentum transport is envisaged as the result of the interaction of turbulent eddies of typical size equal to the disc scale-height,  $H$ , on a turnover time of the order of  $H/c_s$ , where  $c_s$  is the isothermal sound speed. The parameter alpha is often assumed to be constant and smaller than unity. In the presence of a shear background, the vertically integrated stress is then given by

$$\bar{T}_{r\phi}^v = -\alpha \bar{P} \frac{d \ln \Omega}{d \ln r}, \quad (6)$$

where  $\bar{P} = \Sigma c_s^2 / \gamma$  stands for the average pressure,  $\gamma$  is the ratio of specific heats, and we have used the fact that the scale-height of a thin disc in vertical hydrostatic equilibrium is roughly  $H \sim c_s / \Omega$ . This parametrization of the coefficient of turbulent kinematic viscosity implies that the efficiency with which angular momentum is transported is proportional to the local average pressure. This is the idea behind the standard alpha-disc model.

It is worth mentioning that the expression usually employed to define the stress in alpha-models, i.e.,  $\bar{T}_{r\phi}^v = \alpha \bar{P}$ , only provides the correct order of magnitude for the stress in terms of the pressure for a Keplerian discs. Indeed, in this case, the shear parameter

$$q \equiv -\frac{d \ln \Omega}{d \ln r}, \quad (7)$$

is equal to  $3/2 \sim 1$ . However, the fact that the viscous stress is proportional to the local shear cannot be overlooked in regions of the disc where the local angular velocity can differ significantly from its Keplerian value<sup>1</sup>. This is expected to be the case in the boundary layer around an accreting star or close to the marginally stable orbit around a black hole. These inner disc regions are locally characterized by different, and possibly negative, shearing parameters  $q$ . More importantly, if the explicit dependence of the stress on the local shear is not considered then equation (6) predicts unphysical, non-vanishing stresses for solid body rotation,  $q \equiv 0$  (c.f., Blaes 2004).

More than a decade after the paper by Balbus & Hawley (1991), the MRI stands as the most promising driver of the turbulence thought to enable the accretion process. The stresses associated with this MRI-driven turbulence have long been considered as the physical mechanism behind the enhanced turbulent viscosity postulated in the standard model for shear-driven angular momentum transport. It is important to note, however, that there is no a priori reason to assume that the correlated fluctuations defining the total turbulent stress in MRI-driven turbulence are linearly proportional to the local shear. In fact, this assumption can be challenged on both theoretical and numerical grounds.

<sup>1</sup> Also note that it is the explicit linear dependence of the stress on the local shear what gives the equation for angular momentum transport its diffusive nature in standard accretion disc models.

### 3 PREDICTIONS FROM STRESS MODELLING

There are currently few models that aim to describe the local dynamics of turbulent stresses in differentially rotating magnetized media by means of high-order closure schemes (Kato & Yoshizawa 1993, 1995; Ogilvie 2003; Pessah, Chan, & Psaltis 2006b)<sup>2</sup>. In these models, the total stress,  $\bar{T}_{r\phi} = \bar{R}_{r\phi} - \bar{M}_{r\phi}$ , is not prescribed, as in equation (6), but its value is calculated considering the local energetics of the turbulent flow. This is achieved by deriving a set of non-linear coupled equations for the various components of the Reynolds and Maxwell stress tensors. These equations involve unknown triple-order correlations among fluctuations making necessary the addition of ad hoc closure relations.

Although the available models differ on the underlying physical mechanisms that drive the turbulence and lead to saturation, some important characteristics of the steady flows that they describe are qualitatively similar. In particular, all of the models predict that turbulent kinetic/magnetic cells in magnetized Keplerian discs are elongated along the radial/azimuthal direction, i.e.,  $\bar{R}_{rr} > \bar{R}_{\phi\phi}$  while  $\bar{M}_{\phi\phi} > \bar{M}_{rr}$ . Furthermore, turbulent angular momentum transport is mainly carried by correlated magnetic fluctuations, rather than by their kinetic counterpart, i.e.,  $-\bar{M}_{r\phi} > \bar{R}_{r\phi}$ . All of these properties are in general agreement with local numerical simulations. However, a distinctive quantitative feature of these models that concerns us here is that they make rather different predictions for how the stresses depend on the magnitude and sign of the angular velocity gradient.

In the remaining of this section, we highlight the most relevant physical properties characterizing the various models and assess the functional dependence of the total stress,  $\bar{T}_{r\phi}$ , on the sign and steepness of the local angular velocity profile. For convenience, we summarize in Appendix A the various sets of equations that define each of the models.

#### 3.1 Kato & Yoshizawa 1995's Model

In a series of papers, Kato & Yoshizawa (1993, 1995) developed a model for hydromagnetic turbulence in accretion discs with no large scale magnetic fields (see Kato, Fukue, & Mineshige 1998, for a review, and Nakao 1997 for the inclusion of large scale radial and toroidal fields). In their closure scheme, triple-order correlations among fluctuations in the velocity and magnetic fields are modeled in terms of second-order correlations using the two-scale direct interaction approximation (Yoshizawa 1985; Yoshizawa, Itoh, & Itoh 2003), as well as mixing length concepts.

In the model described in Kato & Yoshizawa (1995), the shear parameter  $q$  appears explicitly only in the terms that drive the algebraic growth of the turbulent stresses. The physical mechanism that allows the stresses to grow is the shearing of magnetic field lines. This can be seen by ignoring all the terms that connect the dynamical evolution of the Reynolds and Maxwell stresses. When this is the case, the dynamics of these two quantities are decoupled. The Maxwell stress exhibits algebraic growth while the Reynolds stress oscillates if the flow is Rayleigh stable (i.e.,  $q < 2$ ). The growth of the magnetic stresses is communicated to the different compo-

<sup>2</sup> The studies described here concern models for the evolution of the various correlated fluctuations relevant for describing the dynamics of a turbulent magnetized flow. We note that Vishniac & Brandenburg (1997) proposed an incoherent dynamo model for the transport of angular momentum driven by the generation of large-scale radial and toroidal magnetic fields.

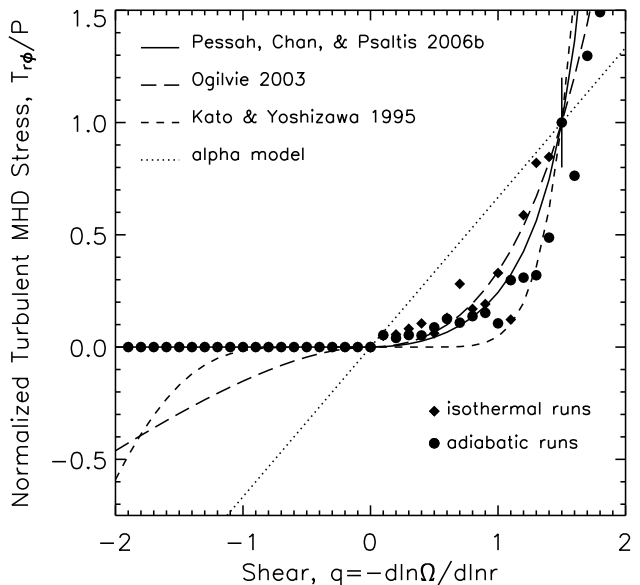


**Figure 1.** Total dimensionless turbulent stress at saturation as a function of the shear parameter  $q \equiv -d \ln \Omega / d \ln r$ . The various lines show the predictions corresponding to the three models for turbulent MHD angular momentum transport discussed in §3. The data points correspond to the volume and time averaged MHD stresses calculated from the series of shearing box simulations described in §4. The diamonds and circles represent the results obtained in the isothermal ( $\gamma = 1$ ) and adiabatic ( $\gamma = 5/3$ ) cases, respectively. The vertical bar in the simulations corresponding to the shear parameter  $q = 3/2$  shows the rms spread in the stresses as calculated from ten numerical simulations for a Keplerian disc. This spread, of roughly 20%, can be taken as a representative value for the typical rms spread in runs with different values of the parameter  $q$  for both the isothermal and adiabatic cases. The dotted line corresponds to a linear relationship between the stresses and the local shear, like the one assumed in the standard model for viscous angular momentum transport. All the quantities in the figure are normalized to unity for a Keplerian profile, i.e., for  $q = 3/2$ .

nents of the Reynolds stress via the tensor  $\bar{S}_{ij} \equiv C_1^S \bar{R}_{ij} - C_2^S \bar{M}_{ij}$ , where  $C_1^S$  and  $C_2^S$  are model constants.

A characteristic feature of this model is that the physical mechanism that leads to saturation is conceived as the escape of magnetic energy in the vertical direction. This process is incorporated phenomenologically by accounting for the leakage of magnetic energy with terms of the form  $-\beta \bar{M}_{ij}$ , where  $\beta$  stands for the escape rate. Although turbulent kinetic and magnetic dissipation act as sink terms in the equations for the various stress components (proportional to the model parameters  $\epsilon_G$  and  $\epsilon_M$ , respectively), if it were not for the terms accounting for magnetic energy escape, the system of equations would be linear. This means that, in order for a stable steady-state solution to exist, either the initial conditions or the constants defining the model will have to be fine-tuned.

The functional dependence of the total stress on the shear parameter  $q$  for the model proposed in Kato & Yoshizawa (1995) is shown in Figure 1. The model predicts vanishingly small stresses for small values of  $|q|$ ; the total stress  $\bar{T}_{r\phi}$  is a very strong function of the parameter  $q$ . Indeed, for  $q > 0$ , the model predicts  $\bar{T}_{r\phi} \sim q^8$ .

#### 3.2 Ogilvie 2003's Model

Based on a set of fundamental principles constraining the non-linear dynamics of turbulent flows, Ogilvie (2003) developed a model for the dynamical evolution of the Maxwell and Reynolds

stresses. Five non-linear terms accounting for key physical processes in turbulent media are modeled by considering the form of the corresponding triple-order correlations, energy conservation, and other relevant symmetries.

The resulting model describes the development of turbulence in hydrodynamic as well as in magnetized non-rotating flows. An interesting feature is that, depending on the values of some of the model constants, it can develop steady hydrodynamic turbulence in rotating shearing flows. For differentially rotating magnetized flows with no mean magnetic fields, the physical mechanism that allows the stresses to grow algebraically is the shearing of magnetic field lines, as in the case of Kato & Yoshizawa (1995). The transfer of energy between turbulent kinetic and magnetic field fluctuations is mediated by the tensor  $c_3 \bar{M}^{1/2} \bar{M}_{ij} - c_4 \bar{R}^{-1/2} \bar{M} \bar{R}_{ij}$ , where  $\bar{R}$  and  $\bar{M}$  are the traces of the Reynolds and Maxwell stresses, respectively, and  $c_3$  and  $c_4$  are model constants. Note that, in this case, the terms that lead to communication between the different Reynolds and Maxwell stress components are intrinsically non-linear. The terms leading to saturation are associated with the turbulent dissipation of kinetic and magnetic energy and are given by  $-c_1 \bar{R}^{1/2} \bar{R}_{ij}$  and  $-c_5 \bar{M}^{1/2} \bar{M}_{ij}$ , respectively.

The dependence of the total stress on the shear parameter for the model described in Ogilvie (2003) is shown in Figure 1. For angular velocity profiles satisfying  $0 < q < 2$ , the stress behaves as  $\bar{T}_{r\phi} \sim q^n$  with  $n$  between roughly 2 and 3. Although the functional dependence of the total stress on negative values of the shear parameter  $q$  is different from the one predicted by the model described in Kato & Yoshizawa (1995), this model also generates MHD turbulence characterized by negative stresses for angular velocity profiles increasing outwards.

### 3.3 Pessah, Chan, & Psaltis 2006's Model

Motivated by the similarities exhibited by the linear regime of the MRI and the fully developed turbulent state (Pessah, Chan, & Psaltis 2006a), we have recently developed a local model for the growth and saturation of the Reynolds and Maxwell stresses in turbulent flows driven by the magnetorotational instability (Pessah, Chan, & Psaltis 2006b). Using the fact that the modes with vertical wave-vectors dominate the fast growth driven by the MRI, we obtained a set of equations to describe the exponential growth of the different stress components. By proposing a simple phenomenological model for the triple-order correlations that lead to the saturated turbulent state, we showed that the steady-state limit of the model describes successfully the correlations among stresses found in numerical simulations of shearing boxes (Hawley, Gammie, & Balbus 1995).

In the model described in Pessah, Chan, & Psaltis (2006b), a new set of correlations couple the dynamical evolution of the Reynolds and Maxwell stresses and play a key role in developing and sustaining the magnetorotational turbulence. In contrast to the two previous cases, the tensor connecting the dynamics of the Reynolds and Maxwell stresses cannot be written in terms of  $\bar{R}_{ij}$  or  $\bar{M}_{ij}$ . This makes it necessary to incorporate additional dynamical equations for these new correlations. In this model, all the second-order correlations exhibit exponential (as opposed to algebraic) growth for shear parameters  $0 < q < 2$ , in agreement with numerical simulations. Incidentally, this is the only case in which the shear parameter,  $q$ , plays an explicit role in connecting the dynamics of the Reynolds and Maxwell stresses. The terms that lead to non-linear saturation are proportional to  $-(\bar{M}/\bar{M}_0)^{1/2}$ , where

$\bar{M}$  is the trace of the Maxwell stress and  $\bar{M}_0$  is a characteristic energy density set by the local disc properties.

The functional dependence of the total turbulent stress on the local shear for the model developed in Pessah, Chan, & Psaltis (2006b) is shown in Figure 1. For angular velocity profiles decreasing outwards, i.e., for  $q > 0$ , the stress behaves like  $\bar{T}_{r\phi} \sim q^n$  with  $n$  between roughly 3 and 4. For angular velocity profiles increasing outwards, i.e., for  $q < 0$ , the stress vanishes identically. Note that this is the only model that is characterized by the absence of transport for all negative values of the shear parameter  $q$ .

It is worth mentioning that in all three high-order closure schemes described above, the pressure,  $\bar{P}$ , does not appear explicitly in the equations defining the models. However, it does play a role in setting the overall scale at which the stresses saturate. This is because the pressure provides a characteristic velocity (e.g., the sound speed) or a characteristic length (e.g., the disc scale height) which in turn determine the saturation level of the stresses  $\bar{T}_{r\phi}$ . In order to compare the predictions of how the dimensionless stresses depend on the local shear independently of other factors, we normalized the quantity  $\bar{T}_{r\phi}/\bar{P}$  predicted by each model in Figure 1 with the values corresponding to the Keplerian cases with the same pressure<sup>3</sup>.

Figure 1 illustrates the sharp contrast between the functional dependence of the saturated stresses predicted by all three MHD models with respect to the standard shear viscous stress defined in equation (5). It is remarkable that, despite the fact that the various models differ on their detailed structure, all of them predict a much steeper functional dependence of the stresses on the local shear. Indeed, for angular velocity profiles decreasing outwards, they all imply  $\bar{T}_{r\phi} \sim q^n$  with  $n \gtrsim 2$ . The predictions of the various models differ more significantly for angular velocity profiles increasing outwards. In this case, the models developed in Kato & Yoshizawa (1995) and Ogilvie (2003) lead to negative stresses, while the model developed in Pessah, Chan, & Psaltis (2006b) predicts vanishing stresses.

## 4 RESULTS FROM NUMERICAL SIMULATIONS

There have been only few numerical studies to assess the properties of magnetorotational turbulence for different values of the local shear. Abramowicz, Brandenburg, & Lasota (1996) carried out a series of numerical simulations employing the shearing box approximation to investigate the dependence of turbulent magnetorotational stresses on the shear-to-vorticity ratio. Although the number of angular velocity profiles that they considered was limited, their results suggest that the relationship between the turbulent MHD stresses and the shear is not linear. On the other hand, Hawley, Balbus, & Winters (1999) carried out a series of shearing box simulations varying the shear parameter from  $q = 0.1$  up to  $q = 1.9$  in steps of  $\Delta q = 0.1$  and reported on the dependence of

<sup>3</sup> Note that the model described in Pessah, Chan, & Psaltis (2006b) was developed to account for the correlations among stresses and magnetic energy density at saturation when there is a weak mean magnetic field perpendicular to the disc mid-plane. It is known that, for a given initial magnetic energy density, numerical simulations of MHD turbulent Keplerian shearing flows tend to saturate at higher magnetic energy densities when there is a net vertical magnetic flux (Hawley, Gammie, & Balbus 1996). The normalization chosen in Fig. 1 allows us to compare the shear-dependence of the various models regardless of their initial field configurations.

the Reynolds and Maxwell stresses on the magnitude of the local shear but not on the corresponding dependence of the total stress.

In order to investigate the dependence of MRI-driven turbulent stresses on the sign and magnitude of the local shear, we modified a version of ZEUS-3D to allow for angular velocity profiles increasing outwards (i.e., characterized by shear parameters  $q < 0$ ). ZEUS is a publicly available code and is based on an explicit finite difference algorithm on a staggered mesh. A detailed description of this code can be found in Stone & Norman (1992a,b) and Stone, Mihalas, & Norman (1992).

#### 4.1 The Shearing Box Approximation

The shearing box approximation has proven to be fruitful in studying the local characteristics of magnetorotational turbulence from both the theoretical and numerical points of view. The local nature of the MRI allows us to concentrate on scales much smaller than the scale height of the accretion disc,  $H$ , and regard the background flow as essentially homogeneous in the vertical direction.

In order to obtain the equations describing the dynamics of a compressible MHD fluid in the shearing box limit, we consider a small box centered at the radius  $r_0$  and orbiting the central object in corotation with the disc at the local speed  $v_0 = r_0 \Omega_0 \check{\phi}$ . The shearing box approximation consists of a first order expansion in  $r - r_0$  of all the quantities characterizing the flow. The goal of this expansion is to retain the most important terms governing the dynamics of the MHD fluid in a locally Cartesian coordinate system (see, e.g., Goodman & Xu 1994; Hawley, Gammie, & Balbus 1995). This is a good approximation as long as the magnetic fields involved are subthermal (Pessah & Psaltis 2005). The resulting set of equations is then given by

$$\frac{\partial \rho}{\partial t} + \nabla \cdot (\rho \mathbf{v}) = 0 \quad (8)$$

$$\frac{\partial \mathbf{v}}{\partial t} + (\mathbf{v} \cdot \nabla) \mathbf{v} = -\frac{1}{\rho} \nabla \left( P + \frac{\mathbf{B}^2}{8\pi} \right) + \frac{(\mathbf{B} \cdot \nabla) \mathbf{B}}{4\pi\rho} - 2\Omega_0 \times \mathbf{v} + q\Omega_0^2 \nabla (r - r_0)^2 \quad (9)$$

$$\frac{\partial \mathbf{B}}{\partial t} = \nabla \times (\mathbf{v} \times \mathbf{B}) \quad (10)$$

$$\frac{\partial E}{\partial t} + \nabla \cdot (E \mathbf{v}) = -P \nabla \cdot \mathbf{v} \quad (11)$$

where  $\rho$  is the density,  $\mathbf{v}$  is the velocity,  $\mathbf{B}$  is the magnetic field,  $P$  is the gas pressure, and  $E$  is the internal energy density. In writing this set of equations, we have neglected the vertical component of gravity and defined the local Cartesian differential operator,

$$\nabla \equiv \check{r} \frac{\partial}{\partial r} + \frac{\check{\phi}}{r_0} \frac{\partial}{\partial \phi} + \check{z} \frac{\partial}{\partial z}, \quad (12)$$

where  $\check{r}$ ,  $\check{\phi}$ , and  $\check{z}$  are, coordinate-independent, orthonormal basis vectors corotating with the background flow at  $r_0$ . Note that the third and fourth terms on the right hand side of equation (9) account for the Coriolis force, present in the rotating frame, and the radial component of the tidal field, respectively. We close the set of equations (8)–(11) by assuming an ideal gas law with  $P = (\gamma - 1)E$ .

#### 4.2 Numerical Set Up

We set the radial, azimuthal, and vertical dimensions of the simulation domain to  $L_r = 1$ ,  $L_\phi = 6$ , and  $L_z = 1$  and consider a grid of  $32 \times 192 \times 32$  zones. This resolution corresponds to the standard resolution used in most shearing box simulations

carried out up to date (see, e.g., Hawley, Gammie, & Balbus 1995; Sano, Inutsuka, Turner, & Stone 2004).

The density scale in the shearing box is arbitrary and we choose  $\rho_0 = 1$  as in, e.g., Hawley, Gammie, & Balbus (1995) and Sano, Inutsuka, Turner, & Stone (2004). We consider the case of zero net magnetic flux through the vertical boundaries<sup>4</sup> by defining the initial magnetic field according to  $\mathbf{B} = B_0 \sin[2\pi(r - r_0)/L_r] \check{z}$ . The plasma  $\beta$  in all the simulations that we perform is  $\beta = P/(B_0^2/8\pi) = 200$ , so the magnetic field is highly subthermal in the initial state. The initial velocity field that corresponds to the steady state solution is  $\mathbf{v} = -q\Omega_0(r - r_0)\check{\phi}$  and we choose the value  $\Omega_0 = 10^{-3}$  in order to set the time scale in the shearing box. Note that for  $q = 3/2$ , this velocity field is simply the first order expansion of a steady Keplerian disc around  $r_0$ . In order to excite the MRI, we introduce random perturbations at the 0.1% level in every grid point over the background internal energy and velocity field in all of the cases.

#### 4.3 Results

Keeping all the numerical settings unchanged, we perform two suites of numerical simulations with different values of the shear parameter  $q$ , from  $q = -1.9$  up to  $q = 1.9$  in steps of  $\Delta q = 0.1$ . The two sets of runs differ only in the value of the adiabatic index  $\gamma$ ; we considered an isothermal case, with  $\gamma = 1.001$ , and an adiabatic case, with  $\gamma = 5/3$ . For each value of the shear parameter  $q$ , we run each simulation for 150 orbits. We then compute a statistically meaningful value for the saturated stress  $\bar{T}_{r\phi}$  and pressure  $\bar{P}$  by averaging the last 100 orbits in each simulation (Winters, Balbus, & Hawley 2003; Sano, Inutsuka, Turner, & Stone 2004).

Figure 1 shows the dimensionless stress  $\bar{T}_{r\phi}/\bar{P}$  obtained for both the isothermal and the adiabatic cases (represented with diamonds and circles respectively) as a function of the local shear. It is evident from this figure that the turbulent magnetorotational stresses are not proportional to the local shear in either the isothermal or the adiabatic cases. There is indeed a strong contrast with respect to the standard assumption of a linear relationship between the stresses and the local shear (dotted line in the same figure) for both positive and negative shear profiles. For angular velocity profiles that decrease with increasing radius, i.e., for  $q > 0$ , all of the turbulent states are characterized by positive mean stresses and thus by outward transport of angular momentum. In these cases, stronger shear results in larger saturated stresses but the functional dependence of the total stress on the local shear is not linear. For angular velocity profiles that increase with increasing radius, i.e., for  $q < 0$ , all the numerical simulations reach the same final state regardless of the magnitude of the shear parameter  $q$ . The stresses resulting from the initial seed perturbations (at the 0.1% level) quickly decay to zero. This is in sharp contrast with the large negative stresses that are implied by the standard Newtonian model for the shear viscous stress in equations (5) and (6).

<sup>4</sup> After submitting this paper we became aware of the impact of numerical resolution on the saturated stresses in Keplerian shearing boxes with zero-net flux. Pessah, Chan, & Psaltis (2007), see also Fromang & Papaloizou (2007), have shown that the saturation of the MRI in this type of simulations depends linearly on the numerical resolution. The numerical results in Figure 1 are normalized with respect to the Keplerian case ( $q = 1.5$ ). Note that the explicit functional dependence of the dimensionless stress on the shear, as shown in Figure 1, assumes that resolution affects all the simulations in the same way, regardless of the value of the shear  $q$ .

In order to explore further the decay of MHD turbulence found for angular velocity profiles increasing outwards, we also performed the following numerical experiment. We seeded a run with a shear parameter  $q = -3/2$  with perturbations at the 100% level of the background internal energy and velocity field. In this case, the timescale for the decay of the initial turbulent state was longer than the one observed in the corresponding run seeded with perturbations at the 0.1% level. The final outcome was nonetheless the same. After a few orbits, the stresses decayed sharply and remained vanishingly small until the end of the run at 150 orbits. This result highlights the strong stabilizing effects of a positive angular velocity gradient on the dynamical evolution of the turbulent stresses due to tangled magnetic fields. This behavior can be understood in terms of the joint restoring action due to magnetic tension and Coriolis forces acting on fluid elements displaced from their initial orbits.

## 5 DISCUSSION AND IMPLICATIONS

In this paper, we investigated the dependence of the turbulent stresses responsible for angular momentum transport in differentially rotating, magnetized media on the local shear as parametrized by  $q = -d \ln \Omega / d \ln r$ . The motivation behind this effort lies in understanding whether one of the fundamental assumptions on which much of the standard accretion disc theory rests, i.e., the existence of a linear relationship between these two quantities, holds when the MHD turbulent state is driven by the MRI. We addressed this problem both in the context of current theoretical turbulent stress models as well as using the publicly available three-dimensional numerical code ZEUS.

From the theoretical point of view, we have seen that, despite their different structures, all of the available high-order closure schemes (Kato & Yoshizawa 1993, 1995; Ogilvie 2003; Pessah, Chan, & Psaltis 2006b) predict stresses whose functional dependence on the local shear differ significantly from the standard model for angular momentum transport. In order to settle this result on firmer grounds, we performed a series of numerical simulations of MRI-driven turbulence in the shearing box approximation for different values of the local shear characterizing the background flow. The main conclusion to be drawn from our study is that turbulent MHD stresses in differentially rotating flows are not linearly proportional to the local background disc shear. This finding challenges one of the central assumptions in standard accretion disc theory, i.e., that the total stress acting on a fluid element in a turbulent magnetized disc can be modeled as a (Newtonian) viscous shear stress.

We find that there is a strong contrast between the stresses produced by MHD turbulence and the viscous shear stresses regardless of whether the disc angular velocity decreases or increases outwards. In the former case, i.e., for  $q > 0$  as in a Keplerian disc, the total turbulent stress generated by tangled magnetic fields is not linearly proportional to the local shear,  $q$ , as it is assumed in standard accretion disc theory. On the other hand, for angular velocity profiles increasing outwards, i.e., for  $q < 0$  as in the boundary layer close to a slowly rotating accreting stellar object, MHD turbulence driven by the MRI fails to transport angular momentum, while viscous shear stresses lead to enhanced negative stresses.

The functional dependence of the local stress on the shear profile determines the topology of transonic accretion flows onto black holes and the radial position of the corresponding critical points (Abramowicz & Kato 1989; Kato, Fukue, & Mineshige

1998; Afshordi & Paczynski 2003). It also plays a critical role in determining the global structure of accretion flows onto stellar objects, determining the exchange of angular momentum between the disc and the gravitating body and even the angular velocity distribution itself (Popham & Narayan 1991). If magnetorotational turbulence is the main mechanism enabling angular momentum transport in accretion discs then the dependence of the stress on the local shear discussed in this paper can have important implications for the global structure and long term evolution of accretion disc around proto-stars, proto-neutron stars, accreting binaries, and active galactic nuclei.

## ACKNOWLEDGMENTS

We are grateful to Jim Stone for useful discussions and for helping us with the necessary modifications to the ZEUS code. We thank Gordon Ogilvie for his detailed comments on an earlier version of this manuscript. We have also benefited with fruitful discussions with Eric Blackman, Omer Blaes, Phil Armitage, and Andrew Cumming on different aspects of stress modelling and accretion theory. We also thank an anonymous referee for useful comments and constructive criticisms. MEP was supported through a Jamieson Fellowship at the Astronomy Department at the UA during part of this study. This work was partially supported by NASA grant NAG-513374.

## APPENDIX A: HIGH-ORDER CLOSURE MODELS

We summarize here the various sets of equations defining the models described in §3. In order to simplify the comparison between the different models, we adopt the notation introduced in §2, even if this was not the original notation used by the corresponding authors. With the same motivation, we work with dimensionless sets of equations obtained by using the inverse of the local angular frequency ( $\Omega_0^{-1}$ ) as the unit of time and the relevant characteristics speeds or lengths involved in each case. We also provide here the values of the various model constants that were adopted in order to obtain the total turbulent stresses as a function of the local shear shown in Figure 1.

### A1 Kato & Yoshizawa 1995' s Model

The model defined by Kato & Yoshizawa is based on the two-scale direct interaction approximation (Yoshizawa 1985; Yoshizawa, Itoh, & Itoh 2003). The temporal evolution of the Reynolds and Maxwell stresses is described by

$$\begin{aligned}
 \partial_t \bar{R}_{rr} &= 4\bar{R}_{r\phi} + \bar{\Pi}_{rr} - \bar{S}_{rr} - \frac{2}{3}\epsilon_G, \\
 \partial_t \bar{R}_{r\phi} &= (q-2)\bar{R}_{rr} + 2\bar{R}_{\phi\phi} + \bar{\Pi}_{r\phi} - \bar{S}_{r\phi}, \\
 \partial_t \bar{R}_{\phi\phi} &= 2(q-2)\bar{R}_{r\phi} + \bar{\Pi}_{\phi\phi} - \bar{S}_{\phi\phi} - \frac{2}{3}\epsilon_G, \\
 \partial_t \bar{R}_{zz} &= \bar{\Pi}_{zz} - \bar{S}_{zz} - \frac{2}{3}\epsilon_G, \\
 \partial_t \bar{M}_{rr} &= \bar{S}_{rr} - 2\beta\bar{M}_{rr} - \frac{2}{3}\epsilon_M, \\
 \partial_t \bar{M}_{r\phi} &= -q\bar{M}_{rr} + \bar{S}_{r\phi} - 2\beta\bar{M}_{r\phi}, \\
 \partial_t \bar{M}_{\phi\phi} &= -2q\bar{M}_{r\phi} + \bar{S}_{\phi\phi} - 2\beta\bar{M}_{\phi\phi} - \frac{2}{3}\epsilon_M, \\
 \partial_t \bar{M}_{zz} &= \bar{S}_{zz} - 2\beta\bar{M}_{zz} - \frac{2}{3}\epsilon_M,
 \end{aligned}$$

where the relevant characteristic speed used to define dimensionless variables is the local sound speed.

In this model, the flow of turbulent energy from kinetic to magnetic field fluctuations is determined by the tensor

$$\bar{S}_{ij} = C_1^S \bar{R}_{ij} - C_2^S \bar{M}_{ij}, \quad (\text{A1})$$

where  $C_1^S$  and  $C_2^S$  are model constants. This quantity plays the most relevant role in connecting the dynamics of the different components of the Reynolds and Maxwell tensors. If  $\bar{S}_{ij}$  is positive, the interactions between the turbulent fluid motions and tangled magnetic fields enhances the latter. The pressure-strain tensor is modeled in the framework of the two scale direct interaction approximation according to

$$\begin{aligned} \bar{\Pi}_{ij} = & -C_1^\Pi (\bar{R}_{ij} - \delta_{ij} \bar{R}/3) - C_2^\Pi (\bar{M}_{ij} - \delta_{ij} \bar{M}/3) \\ & - q C_0^\Pi \bar{R} (\delta_{ir} \delta_{jr} + \delta_{i\phi} \delta_{j\phi}), \end{aligned} \quad (\text{A2})$$

where  $\bar{R}$  and  $\bar{M}$  stand for the traces of the Reynolds and Maxwell stresses, respectively. This tensor accounts for the redistribution of turbulent kinetic energy along the different directions and tends to make the turbulence isotropic. The dissipation rates are estimated using mixing length arguments and are modeled according to

$$\epsilon_G = \frac{3}{2} \nu_G (\bar{R} + \bar{M}), \quad (\text{A3})$$

$$\epsilon_M = \frac{3}{2} \nu_M (\bar{R} + \bar{M}), \quad (\text{A4})$$

where  $\nu_G$  and  $\nu_M$  are dimensionless constants. The escape of magnetic energy in the vertical direction is taken into account phenomenologically via the terms proportional to the (dimensionless) rate  $\beta = X \bar{M}^{1/2}$ , with  $0 < X < 1$ .

The values of the constants that we considered in order to obtain the curve shown in Figure 1 are the same as the ones considered in case 2 in Kato & Yoshizawa (1995), i.e.,  $C_0^\Pi = C_1^\Pi = C_2^\Pi = C_1^S = C_2^S = 0.3$ ,  $\nu_G = \nu_M = 0.03$ . We further consider  $X = 0.5$  as a representative case.

## A2 Ogilvie 2003's Model

Ogilvie proposed that the functional form of the equations governing the local, non-linear dynamics of a turbulent MHD flow are strongly constrained by a set of fundamental principles. The model that he developed is given by the following set of equations

$$\begin{aligned} \partial_t \bar{R}_{rr} &= 4\bar{R}_{r\phi} - c_1 \bar{R}^{1/2} \bar{R}_{rr} - c_2 \bar{R}^{1/2} (\bar{R}_{rr} - \bar{R}/3) \\ &\quad + c_3 \bar{M}^{1/2} \bar{M}_{rr} - c_4 \bar{R}^{-1/2} \bar{M} \bar{R}_{rr}, \\ \partial_t \bar{R}_{r\phi} &= (q-2) \bar{R}_{rr} + 2\bar{R}_{\phi\phi} - (c_1 + c_2) \bar{R}^{1/2} \bar{R}_{r\phi} \\ &\quad + c_3 \bar{M}^{1/2} \bar{M}_{r\phi} - c_4 \bar{R}^{-1/2} \bar{M} \bar{R}_{r\phi}, \\ \partial_t \bar{R}_{\phi\phi} &= 2(q-2) \bar{R}_{r\phi} - c_1 \bar{R}^{1/2} \bar{R}_{\phi\phi} - c_2 \bar{R}^{1/2} (\bar{R}_{\phi\phi} - \bar{R}/3) \\ &\quad + c_3 \bar{M}^{1/2} \bar{M}_{\phi\phi} - c_4 \bar{R}^{-1/2} \bar{M} \bar{R}_{\phi\phi}, \\ \partial_t \bar{R}_{zz} &= -c_1 \bar{R}^{1/2} \bar{R}_{zz} - c_2 \bar{R}^{1/2} (\bar{R}_{zz} - \bar{R}/3) \\ &\quad + c_3 \bar{M}^{1/2} \bar{M}_{zz} - c_4 \bar{R}^{-1/2} \bar{M} \bar{R}_{zz}, \\ \partial_t \bar{M}_{rr} &= c_4 \bar{R}^{-1/2} \bar{M} \bar{R}_{rr} - (c_3 + c_5) \bar{M}^{1/2} \bar{M}_{rr}, \\ \partial_t \bar{M}_{r\phi} &= -q \bar{M}_{rr} + c_4 \bar{R}^{-1/2} \bar{M} \bar{R}_{r\phi} - (c_3 + c_5) \bar{M}^{1/2} \bar{M}_{r\phi}, \\ \partial_t \bar{M}_{\phi\phi} &= -2q \bar{M}_{r\phi} + c_4 \bar{R}^{-1/2} \bar{M} \bar{R}_{\phi\phi} - (c_3 + c_5) \bar{M}^{1/2} \bar{M}_{\phi\phi}, \\ \partial_t \bar{M}_{zz} &= c_4 \bar{R}^{-1/2} \bar{M} \bar{R}_{zz} - (c_3 + c_5) \bar{M}^{1/2} \bar{M}_{zz}. \end{aligned}$$

Here  $\bar{R}$  and  $\bar{M}$  denote the traces of the Reynolds and Maxwell tensors and we have defined the quantities  $c_1, \dots, c_5$  which are related to the positive dimensionless constants defined by Ogilvie

$C_1, \dots, C_5$  via  $C_i = L c_i$ , where  $L$  is a vertical characteristic length (e.g., the thickness of the disc). Note that Ogilvie's original equations are written in terms of Oort's first constant  $A = q/2$  (in dimensionless units).

In this model, the constant  $c_2$  dictates the return to isotropy expected to be exhibited by freely decaying hydrodynamic turbulence. The terms proportional to  $c_3$  and  $c_4$  transfer energy between kinetic and magnetic turbulent fields. The constants  $c_1$  and  $c_5$  are related to the dissipation of turbulent kinetic and magnetic energy, respectively. Note that, in order to obtain the representative behavior of the total turbulent stress as a function of the local shear that is shown Figure 1, we set  $c_1, \dots, c_5 = 1$ .

## A3 Pessah, Chan, & Psaltis 2006's Model

We have recently developed a local model for the growth and saturation of the Reynolds and Maxwell stresses in turbulent flows driven by the magnetorotational instability that leads to exponential growth for the stresses and can account for a number of correlations observed in numerical simulations (Pessah, Chan, & Psaltis 2006b). In this model, the Reynolds and Maxwell stresses are not only coupled by the same linear terms that drive the turbulent state in the previous two models but there is also a new tensorial quantity that couples their dynamics further. This new tensor cannot be written in terms of  $\bar{R}_{ij}$  or  $\bar{M}_{ij}$ , making it necessary to incorporate additional dynamical equations.

The set of equations defining this model is

$$\begin{aligned} \partial_t \bar{R}_{rr} &= 4\bar{R}_{r\phi} + 2\bar{W}_{r\phi} - \sqrt{\frac{\bar{M}}{M_0}} \bar{R}_{rr}, \\ \partial_t \bar{R}_{r\phi} &= (q-2) \bar{R}_{rr} + 2\bar{R}_{\phi\phi} - \bar{W}_{rr} + \bar{W}_{\phi\phi} - \sqrt{\frac{\bar{M}}{M_0}} \bar{R}_{r\phi}, \\ \partial_t \bar{R}_{\phi\phi} &= 2(q-2) \bar{R}_{r\phi} - 2\bar{W}_{\phi r} - \sqrt{\frac{\bar{M}}{M_0}} \bar{R}_{\phi\phi}, \\ \partial_t \bar{W}_{rr} &= q\bar{W}_{r\phi} + 2\bar{W}_{\phi r} + \zeta^2 k_{\max}^2 (\bar{R}_{r\phi} - \bar{M}_{r\phi}) - \sqrt{\frac{\bar{M}}{M_0}} \bar{W}_{rr}, \\ \partial_t \bar{W}_{r\phi} &= 2\bar{W}_{\phi\phi} - \zeta^2 k_{\max}^2 (\bar{R}_{rr} - \bar{M}_{rr}) - \sqrt{\frac{\bar{M}}{M_0}} \bar{W}_{r\phi}, \\ \partial_t \bar{W}_{\phi r} &= (q-2) \bar{W}_{rr} + q\bar{W}_{\phi\phi} \\ &\quad + \zeta^2 k_{\max}^2 (\bar{R}_{\phi\phi} - \bar{M}_{\phi\phi}) - \sqrt{\frac{\bar{M}}{M_0}} \bar{W}_{\phi r}, \\ \partial_t \bar{W}_{\phi\phi} &= (q-2) \bar{W}_{r\phi} - \zeta^2 k_{\max}^2 (\bar{R}_{r\phi} - \bar{M}_{r\phi}) - \sqrt{\frac{\bar{M}}{M_0}} \bar{W}_{\phi\phi}, \\ \partial_t \bar{M}_{rr} &= -2\bar{W}_{r\phi} - \sqrt{\frac{\bar{M}}{M_0}} \bar{M}_{rr}, \\ \partial_t \bar{M}_{r\phi} &= -q \bar{M}_{rr} + \bar{W}_{rr} - \bar{W}_{\phi\phi} - \sqrt{\frac{\bar{M}}{M_0}} \bar{M}_{r\phi}, \\ \partial_t \bar{M}_{\phi\phi} &= -2q \bar{M}_{r\phi} + 2\bar{W}_{\phi r} - \sqrt{\frac{\bar{M}}{M_0}} \bar{M}_{\phi\phi}, \end{aligned}$$

where we have defined dimensionless variables considering the mean Alfvén speed  $\bar{v}_{Az} = \bar{B}_z / \sqrt{4\pi\rho_0}$ , with  $\bar{B}_z$  the local mean magnetic field in the vertical direction and  $\rho_0$  the local disc density. The tensor  $\bar{W}_{ik} = \langle \delta v_i \delta j_k \rangle$  is defined in terms of correlated

fluctuations in the velocity and current ( $\delta j = \nabla \times \delta B$ ) fields. The (dimensionless) wavenumber defined as

$$k_{\max}^2 = q - \frac{q^2}{4} \quad (\text{A5})$$

corresponds to the scale at which the MRI-driven fluctuations exhibit their maximum growth and

$$\bar{M}_0 \equiv \xi \rho_0 H \Omega_0 \bar{v}_{Az}, \quad (\text{A6})$$

is a characteristic energy density set by the local disc properties, with  $H$  the disc thickness. The parameters  $\zeta \simeq 0.3$  and  $\xi \simeq 11$  are model constants which are determined by requiring that the Reynolds and Maxwell stresses satisfy the correlations observed in numerical simulations of Keplerian shearing boxes with  $q = 3/2$  (Hawley, Gammie, & Balbus 1995).

## REFERENCES

- Abramowicz M., Brandenburg A., Lasota J.P., 1996, MNRAS, 281, L21
- Abramowicz M., Kato S., 1989, ApJ, 336, 304
- Afshordi N., Mukhopadhyay B., Narayan R., 2005, ApJ, 629, 373
- Afshordi N., Paczynski B., 2003, ApJ, 592, 354
- Armitage P.J., 1998, ApJ, 501, L189
- Balbus S.A., 2003, ARA&A, 41, 555
- Balbus S.A., Hawley J.F., 1991, ApJ, 376, 214
- Balbus S.A., Hawley J.F., Stone, J.M., 1996, ApJ, 467, 76
- Balbus S.A., Hawley J.F., 1997, ASPC, 121, 90
- Balbus S.A., Hawley J.F., 1998, Rev. Mod. Phys., 70, 1
- Balbus S.A., Papaloizou J.C.B., 1999, ApJ, 521, 650
- Balbus S.A., Hawley, J.F., 2006, ApJ, 652, 1020
- Blaes O., 2004, in *Accretion Disks, Jets, and High Energy Phenomena in Astrophysics*, Les Houches Lect. Notes 78, 137-185
- Brandenburg A., 1998, in *Theory of Black Hole Accretion Discs*, Abramowicz M. A., Björnsson G., Pringle J. E., eds, Cambridge Univ. Press, Cambridge, p. 61
- Brandenburg A., 2001, ApJ, 550, 824
- Brandenburg A., Nordlund A., Stein R.F., Torkelsson U., 1995, ApJ, 446, 741
- Frank J., King A., Raine D.J., 2002, *Accretion Power in Astrophysics*, 3rd edn. Cambridge Univ. Press, Cambridge
- Fromang, S., Papaloizou, J., 2007, A&A, submitted [arXiv:0705.3621]
- Gammie C.F., 1998, in *Accretion Processes in Astrophysical Systems: Some Like it Hot!*, S.S., Holt, T.R. Kallman, AIPC 431, 99
- Goodman J., Xu G., 1994, ApJ, 432, 213
- Hawley J.F., 2000, ApJ, 528, 462
- Hawley J.F., 2001, ApJ, 554, 534
- Hawley J.F., Balbus S.A., Winters W.F., 1999, ApJ, 518, 394
- Hawley J.F., Gammie C.F., Balbus S.A., 1995, ApJ, 440, 742
- Hawley J.F., Gammie C.F., Balbus S.A., 1996, ApJ, 464, 690
- Hawley J.F., Krolik J.H., 2001, ApJ, 548, 348
- Ji, H., Burin, M., Schartman, E., Goodman, J. 2006, Nature, 444, 343
- Kato S., Fukue J., Mineshige S., 1998, *Black-Hole Accretion Disks*. Kyoto University Press., Kyoto
- Kato S., Yoshizawa A., 1993, Publ. Astron. Soc. Jap., 45, 103
- Kato S., Yoshizawa A., 1995, Publ. Astron. Soc. Jap., 47, 629
- Landau L.D., Lifshitz E.M., 1959, *Fluid Mechanics*. Pergamon Press. Oxford
- Lynden-Bell D., Pringle J.E., 1974, MNRAS, 168, 603
- Mukhopadhyay B., Afshordi N., Narayan R., 2005, ApJ, 629, 383
- Nakao Y., 1997, Publ. Astron. Soc. Jap., 49, 659
- Ogilvie G.I., 2003, MNRAS, 340, 969
- Pessah M.E., Psaltis D., 2005, ApJ, 628, 879
- Pessah M.E., Chan C.K., Psaltis D., 2006a, MNRAS, 372, 183P
- Pessah M.E., Chan C.K., Psaltis D., 2006b, Phys. Rev. Lett., 97, 221103
- Pessah M.E., Chan C.K., Psaltis D., 2007, ApJ, 668, L51
- Popham R., Narayan R., 1991, ApJ, 370, 604
- Ryu D., Goodman J., 1992, ApJ, 388, 438
- Sano T., Inutsuka S., Turner N.J., Stone J.M., 2004, ApJ, 605, 321
- Shakura N.I., Sunyaev R.A., 1973, A&A, 24, 337
- Stone J.M., Norman M.L., 1992a, ApJS, 80, 753
- Stone J.M., Norman M.L., 1992b, ApJS, 80, 791
- Stone J.M., Mihalas, D., Norman M.L., 1992, ApJS, 80, 819
- Stone J.M., Balbus S.A., 1996, ApJ, 464, 364
- Stone J.M., Pringle J.E., 2001, MNRAS, 322, 461
- Stone J.M., Hawley J.F., Gammie C.F., Balbus S.A., 1996, ApJ, 463, 656
- Vishniac E.T., Brandenburg A., 1997, ApJ, 475, 263
- Winters W.F., Balbus S.A., Hawley J.F., 2003, MNRAS, 340, 519
- Yoshizawa A., 1985, Phys. Fluids, 28, 3313
- Yoshizawa A., Itoh S.I., Itoh K., 2003, *Plasma and Fluid Turbulence: Theory and Modelling*. Institute of Physics, London